Electron-phonon scattering in silver: Surface Landau-level resonance

John W. Mitchell and R. G. Goodrich
Department of Physics and Astronomy, Louisiana State University, Baton Rouge, Louisiana 70803-4001
(Received 24 June 1985)

Measurements of the anisotropic electron-phonon collision frequency on the Fermi surface of Ag are reported for a number of points on the intersection of the Fermi surface with the (100) and (110) central planes and at the neck and ⟨110⟩ point in the (111) plane. Analyses of the temperature-dependent surface Landau-level resonance (SLLR) line shapes are used to obtain the electron-phonon scattering rates at each resonant electron location. The results of this experiment, in conjunction with previous measurements, give a complete picture of the anisotropy of electron-phonon scattering in Ag.

INTRODUCTION

In recent years there have been a number of investigations of the anisotropic electron-phonon scattering rates $\Gamma_p(\mathbf{k})=\gamma(\mathbf{k})T^3$ in the noble metals, copper, silver, and gold. Theoretical calculations of $\gamma(\mathbf{k})$ have been carried out for Cu (Refs 1—3) and all three metals have been the focus of experimental programs employing radio-frequency size effect (RFSE) [Cu (Refs. 4 and 5), Ag (Refs. 6 and 7), and Au (Ref. 8)], surface Landau-level resonance (SLLR) [Cu (Ref. 9)], and most recently time of flight effect (TFE) [Ag (Refs. 10 and 11)] measurements. The results of these investigations confirm the existence of a strongly anisotropic dependence of $\gamma(\mathbf{k})$ on the Fermi-surface (FS) location of the electrons. Both the theoretical and experimental studies agree on the general behavior of the anisotropy, but the details of the magnitude of the anisotropy are not in good agreement. In particular, there are substantial differences between results obtained using the various experimental techniques. These differences are especially apparent in the studies that have been made on Ag. It is the purpose of the present work to present an independent measurement of $\gamma(\mathbf{k})$ at a number of FS locations in Ag in an attempt to resolve some of the existing discrepancies.

The results presented here were derived from measurements of the temperature dependence of surface Landau-level resonance (SLLR) line shapes. In a recent paper[12] we have reported the results of constant-temperature SLLR measurements on Ag and have determined the FS locations as well as the Fermi velocities of the resonant electrons. Doezema and Koch[9,13] (DK) have made an extensive study of the electron-phonon scattering rates in Cu using SLLR and we, in general, follow their technique and notation in this paper.

The electrons contributing to the SLLR signals are located in a small, on the order of 1°, angular range about the $k_z=0$ region on the FS, where k_z is the component of the resonant-electron momentum perpendicular to the sample surface. The width of this angular range depends on the depth and radius of the skipping orbit contributing to the signal. The principal contribution to the signal comes from electrons having an extremal value of the resonance parameter $R=(K/v_F^3)_\perp^{1/2}$, where K is the radius of curvature of the FS in the direction of the orbit and v_F is the Fermi velocity. The symbol $\perp$ indicates that only the components of K and v_F perpendicular to the magnetic field are to be considered. In addition, there are smaller contributions from electrons lying on the $k_z=0$ band on either side of the extremal point. The angular extent of this contributing region depends on the variation of the resonance parameter about its extremal value.

It is expected that a single phonon scattering event will remove an electron from the resonant band with the result that all scattering events are equally effective. In addition, as discussed by DK (Ref. 9) and Prange (Ref. 14), most scattering events will result from collisions with bulk rather than surface phonons. Finally, in the (1.5—10)-K temperature range over which the experiment was performed, electron-phonon scattering will be the dominant temperature-dependent effect. This means the total scattering rate should be of the form

$$\Gamma(\mathbf{k})=\Gamma_0(\mathbf{k})+\gamma(\mathbf{k})T^3 ,$$

where $\Gamma_0(\mathbf{k})$ is the temperature-independent rate due to impurities, lattice defects, and surface roughness or curvature.

EXPERIMENTAL

Basic details of the experimental apparatus and sample preparation were given in Ref. 12 and we describe here only the additional provisions made for varying and measuring the temperature of the sample. Thermal isolation of the microwave cavity was achieved by mounting the copper resonant cavity at the end of a section of thin-wall stainless-steel waveguide within a vacuum can be immersed in liquid ^{4}He. The temperature was adjusted by varying the microwave power incident on the cavity and by using a noninductive heater wound on the outside of the cavity. Overall, long-term temperature stability of better than 0.5% was achieved for the measurements.

Temperatures were measured using an ac bridge to determine the conductance of a carbon thermometer. The thermometer was thermally grounded to an oxygen-free

high-conductivity (OFHC) copper backplate and a phosphor-bronze spring was used to attach the backplate and the Ag sample to the microwave cavity. Care was taken to ensure that all thermometer leads were thermally anchored to the cavity and backplate and that good thermal contact was made between the sample and the backplate. The thermometer was calibrated at 30 points between 1.4 and 15 K using a commercially calibrated germanium thermometer as a standard. The calibration points were fit using a six-term logarithmic series and experimental temperatures were determined from this. Considering calibration, thermal coupling, and instability, the uncertainty in the temperature determination for each resonance curve is approximately 0.5%.

LINE-SHAPE CONSIDERATIONS

Resonance peaks in the first magnetic field derivative of the microwave surface impedance (dR/dH) measured as a function of applied magnetic field are observed in an SLLR experiment. The resulting line shapes are described in the Nee, Koch, and Prange[15] (NKP) skipping-orbit theory by three line-shape fitting parameters: R, β, and Γ^*. The resonance parameter R determines the field position of the resonances while β determines the relative amplitudes of peaks in a particular resonance series. In a previous paper[12] we determined the values of R and β for the observed resonant-electron locations on the Ag FS and take these to be known. The third parameter $\Gamma^*=\Gamma/\omega$ determines the width ΔH_p at half-amplitude and the absolute amplitude of the peak.

DK have used a library of NKP characteristic spectra to find a relationship between the fractional half-width $\Delta H_p/H_p$ and Γ^*, where H_p is the field value of the resonance peak and ΔH_p is the width of the line measured at half-amplitude. Using the (1-2) transition and measuring the amplitude from the low-field side of the resonance line, they found $\Delta H_p/H_p$ to be linear in Γ^* over the range of fractional half-widths characteristic of their experimental values. For a cylindrical FS a relationship $\Delta H_p/H_p=1.51\Gamma^*+0.007$ was found to apply in the range of Γ^* from 0.025 to 0.225. Similarly, for a spherical FS geometry, where the effects of k_H broadening must be considered, $\Delta H_p/H_p$ was found to be linear over the range of Γ^* from 0.025 to 0.150 with $\Delta H_p/H_p=1.56\Gamma^*+0.02$. We have used the same library of NKP spectra and have obtained identical results over these ranges of Γ^*. The Ag FS is locally spherical around most of the points studied and our line-shape analysis uses the calculated spectra typical of a spherical FS. However, while all of the Cu measurements reported by DK fell into the range of Γ^* from 0.025 to 0.15, this was not true for Ag. The resonance lines measured in Ag were typically broader than in Cu and while most of the data fell below $\Delta H_p/H_p=0.254$ ($\Gamma^*=0.15$), some did not. As noted by DK the relationship between $\Delta H_p/H_p$ and Γ^* changes above $\Gamma^*=0.15$ for a spherical FS, but we have found it to be linear in the range $\Gamma^*=0.15$ to 0.3 and expressible as $\Delta H_p/H_p=1.82\Gamma^*-0.018$. In addition, we have examined the relationship of $\Delta H_{(1\text{-}3)}/H_{(1\text{-}3)}$ to Γ^* for the (1-3) transition. Measuring the amplitude of the (1-3) peak from the high-field side we find a linear relationship $\Delta H_{(1\text{-}3)}/H_{(1\text{-}3)}=1.71\Gamma^*+0.005$ in the range of Γ^* from 0.125 to 0.275. We have checked this relationship on lines analyzed using the (1-2) transition with good agreement and have used it in the analysis of one resonance location.

The experimentally obtained value of Γ^* represents a weighted average of the local values of Γ^* over the range of contributing electrons. A calculation of the precise nature of the weighting and of the range over which the average applies requires prior knowledge of the manner in which the values of Γ^* and R vary around the extremal location. The simplest case is that of a cylindrical FS, where both parameters are constant along the $k_z=0$ zone. Here the value of Γ^* is representative of all electrons in the narrow ($\sim 1°$) strip about the $k_z=0$ line. Only slightly more complex is a region of FS where the cross-section parallel to the sample surface is circular and has constant K, v_F, and Γ^*. For small Γ^* the only weighting factors are geometric and the effective range of the contributing electrons is an angle α around the extremal location for which

$$\frac{R_\alpha - R_{\text{ext}}}{R_{\text{ext}}} = \frac{\Delta R}{R_{\text{ext}}} \simeq \frac{\Delta H_p}{H_p} \,. \tag{1}$$

DK have calculated this condition to give an effective strip length on the order of $10^{-1}k_F$ for a typical resonance linewidth $\Delta H/H \simeq 5\%$. Real FS conditions are different to varying degrees from these examples, although for most of the measured FS locations the geometry is locally spherical and so the second example provides a reasonable estimate of the length of the effective band. This estimate must be considered to be an upper limit since the effective strip length calculated in this manner neglects all nongeometric line-broadening factors such as surface, impurity, and defect scattering.

A second consideration is that, for a highly anisotropic $\Gamma(\mathbf{k})$, the length of the effective strip and with it the range of $\Gamma(\mathbf{k})$ values contributing to the linewidth is temperature dependent. The variation in the length of the effective strip can be estimated by examining the effect of temperature changes on the relative magnitudes of contributions to the resonance line shape from FS locations having differing γ. The magnitude of the contribution to the resonance line amplitude from a local region of FS is expected to vary as Γ_L^{-2} (Ref. 16), where Γ_L is the characteristic scattering rate of the local region. However, the temperature dependent part of Γ causes less than a 5% variation in Γ over the (1—10)-K range. This results in a maximum 10% change in the relative amplitudes of local contributing regions over the entire effective band. Since the largest contributions to the overall signal come from electrons near the extremal location the result of a change in effective strip length is expected to be small over the measured temperature range.

This conclusion is supported both by this work and by that reported by DK since a significant dependence of the measured linewidth on small variations in the length of the effective band should cause a deviation from a T^3 dependence of the measured Γ^*. The measured Γ^* values are, in fact, closely T^3 dependent for all measured ex-

tremal FS locations, leading once again to the conclusion that the temperature dependence of the length of the effective strip has little effect on the overall resonance linewidth.

Considering all of these factors, we find that Eq. (1) applied at the lowest measured temperature provides a reasonable estimate of the upper limit of the size of the FS region contributing to the measured resonance linewidth. The value of $\gamma(\mathbf{k})$ determined from analysis of the variation of the experimental linewidths with changes in the sample temperature must be considered as representing an average over this effective region although this averaging does not alter the point character of the measurements to a great extent since the size of the effective region is small.

EXPERIMENTAL RESULTS

As shown in Ref. 12, the actual spectrum obtained for a given magnetic field orientation is a superposition of the individual spectra of electrons at several different FS locations. The identification of these FS locations from the associated magnetic field direction is discussed in Ref. 12. In Ref. 12 only the magnetic field value of the (1-2) [or in one instance (2-3)] transition peak was used in the measurements and the only requirement was that two distinct spectra be separable to the extent that any peak shifts introduced by their overlap were negligible. In this work, considerably more stringent criteria have been adopted. Since Γ^* is found from the width at half-amplitude of the peak being measured, we require that no other peaks have a significant influence on the line shape. This criterion greatly reduces the number of FS locations which can be included for analysis.

At the FS locations where this clean-signal criterion is met we have recorded dR/dH spectra at several temperatures between 1.5 and 10 K. From these experimental curves we measure $\Delta H_p/H_p$ and using the appropriate relation find $\Gamma^*(T)$. As discussed above, we expect the dominant temperature-dependent effect on the line shape to result from single-event scattering between the resonant electrons and bulk thermal phonons, and this is expected to yield a linear dependence of $\Gamma^*(T)$ on T^3. We have plotted our data at representative FS locations against powers of T from T^1 to T^5. Over the temperature range measured we find a straight line in the T^3 plots showing only expected experimental scatter in the data points while other powers of T show varying amounts of consistent nonlinearity. This being the case, we have fitted all data to a linear dependence on T^3 and use the results to find the values of $\gamma(\mathbf{k})=\Gamma_p(\mathbf{k})/T^3$. The resulting values of $\gamma(\mathbf{k})$ at representative FS locations are given in Table I and in Fig. 1. In Table I, as in Ref. 12, the angle θ is the orientation of the external magnetic field, while in both Table I and Fig. 1 the angle ϕ gives the FS location of the resonant electrons.

Also given in Table I are the temperature-independent scattering rate Γ_0 at each location. It should be remembered that Γ_0 includes both the temperature-independent scattering due to the bulk and that due to surface roughness or curvature. The values of Γ_0 given show some variation from location to location on the same sample and considerably more variation between samples. Care should be taken in interpreting the variation in the measured Γ_0 with FS location as reflecting a true anisotropy in the temperature-independent scattering. In fact, the relative consistency of the values of Γ_0 obtained for a particular sample suggests that any such anisotropy is small.

An exception to the above general discussion of line shapes applies to the locations measured in the (111) sample plane. As discussed in Ref. 12, the amplitude of the neck signal was less than that of the other resonances observed in this sample. In addition, there was some interference with the neck signal at all magnetic field orientations with the result that it failed to meet our clean-signal criterion. This failure meant that measurements of

TABLE I. Experimental values of the electron-phonon scattering parameter $\gamma(\mathbf{k})$ and the temperature-independent scattering rate Γ_0. The angle θ is the magnetic field direction measured from the ⟨010⟩ axis in the (100) zone, and from the ⟨110⟩ axis in the (110) and (111) zones. The angle ϕ is the FS location measured from ⟨100⟩ in the (100) and (110) zones and from ⟨112⟩ in the (111) zone.

Zone	θ (deg)	ϕ (deg)	Γ_0 (10^{10} sec^{-1})	γ (10^7 sec^{-1}K^{-3})
(100)	15	4.6	4.58	1.91
	45	10.8	4.13	1.68
(110)	0	0	2.41	1.94
	10	5.6	2.21	1.91
	20	9.0	2.51	1.65
	40	14.2	2.31	1.40
	70	19.3	2.7	0.92
	40	38.6[a]	2.04	1.94
	90	70.2[a]	2.06	3.16
(111)	17	30	6.05	0.37
	neck		2.345	7.1

[a]These measurements were performed after the sample had been removed from the sample holder and remounted.

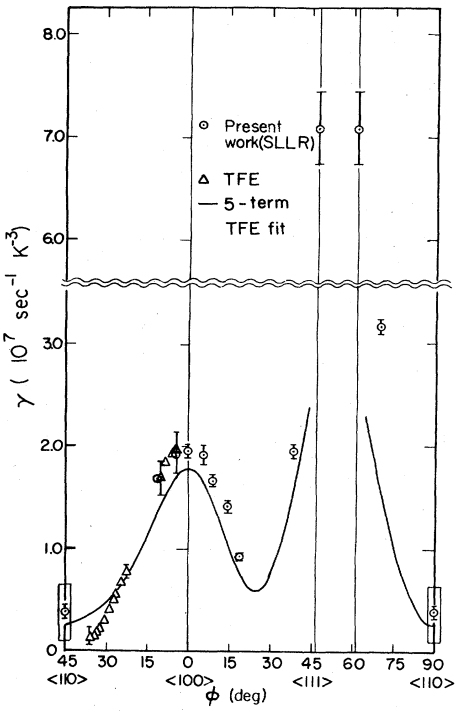

FIG. 1. Anisotropy of the electron-phonon scattering parameter $\gamma(\mathbf{k})$ over the (100) and (110) zones of Ag. The TFE points are taken from the plot in Fig. 4 of Ref. 10. The uncertainty ranges shown for the SLLR points reflect the uncertainty in fitting the measured values of $\Gamma(T)$ to an equation of the form $\Gamma(T)=\Gamma_0+\gamma(\mathbf{k})T^3$. Uncertainty ranges are omitted from the SLLR points at $\phi=4.6°$ and $\phi=10.8°$ for clarity. The boxes around the points shown at $\langle 110\rangle$ reflect the range of $\gamma(\mathbf{k})$ over which they are averaged. The solid line is the five-term inversion of TFE data taken from the plot in Fig. 3 of Ref. 11.

the half-width of this signal could only be obtained by an unfolding procedure. Fortunately, the structure of the overlapping peak proved relatively simple. The interfering peak was found to have a very low characteristic $\gamma(\mathbf{k})$ which allowed its shape to be estimated from data taken at higher temperatures where the effect of the neck peak was negligible. This information was used to extrapolate the shape of the peak to lower temperature and its amplitude in the overlap region was subtracted point by point from the composite amplitude. The result was a plot of the neck signal alone and this was used to find $\gamma(\mathbf{k})$ at the neck. A check on this method can be made by determining $\gamma(\mathbf{k})$ for the interfering peak. This was done both for a range of temperature where the interference for the neck signal was significant, using the extrapolated peak shape, and for the temperature range where the neck signal was negligible. In the lower-temperature range a value of $4.08\times10^6\ \mathrm{sec}^{-1}\mathrm{K}^{-3}$ was calculated for γ, while the value found in the high-temperature range was $3.71\times10^6\ \mathrm{sec}^{-1}\mathrm{K}^{-3}$. These values differ by about 10% which is well within their cumulative uncertainty. Because of the difficulty involved in obtaining usable spectra it proved impossible to investigate any anisotropy in $\gamma(\mathbf{k})$ around the neck.

The resonance line which we have analyzed in performing the unfolding of the neck signal is of considerable interest as well. The amplitude of the resonance associated with $\phi=90°$ ($\langle 110\rangle$) in the (110) sample was quite small and it proved impossible to measure any temperature dependence at this location. As discussed in Ref. 12, however, the principal resonance observed in the (111) plane is associated with a cylinder-like band of electrons near a line connecting the necks on either side of the (111) central plane and containing the $\langle 110\rangle$ point in that plane. The FS is not symmetric about the (111) central plane except at the $\langle 110\rangle$ points with the result that these are the only points on the central plane for which $k_z=0$. As one moves away from $\langle 110\rangle$, the $k_z=0$ point falls near a line between $\langle 110\rangle$ and the nearest $\langle 111\rangle$. This line corresponds to the region of FS in the (110) central plane on either side of $\langle 110\rangle$. For a considerable range around $\langle 110\rangle$ the $k_z=0$ points are cylinder-like in the sense that K, v_F, and R vary slowly. The detected signal is representative of an average over this cylinder-like region. This may explain the approximate factor-of-4 difference in the $\langle 110\rangle$ scattering rate measured in this manner and that extrapolated from TFE measurements since the value of $\gamma(\mathbf{k})$ is expected to change rapidly away from $\langle 110\rangle$ and our signal includes an average over a large range of FS along this line. In Fig. 1 the box around the $\langle 110\rangle$ point represents the predicted range of $\gamma(\mathbf{k})$ entering into the measured average value.

Finally, we consider the assignment of uncertainties to the measured values of $\gamma(\mathbf{k})$. The statistical variations found in the least-squares analysis of the slope of $\Gamma^*(T)$ as a function of T^3 reflect the approximately 0.9% uncertainty in T^3 as well as uncertainties in the measured linewidths and are typically less than 5%. In addition, there is some uncertainty from the use of an idealized spherical FS geometry and constant $\beta=0.5$ in developing the library curves and from their application in finding $\Gamma^*(T)$ from the measured $\Delta H_p/H_p$ without considering in detail the possible differences in k_H broadening at different locations. We estimate these factors to result in a possible additional uncertainty in the measured slopes on the order of 3—6%, depending on the difference between the β value associated with a particular resonance series and 0.5. Combined with the statistical uncertainty in the slopes this yields an overall uncertainty in the measured values of $\gamma(\mathbf{k})$ of 6—8%. The value reported for the neck in the (111) plane has a greater uncertainty associated with it due to the unfolding procedure. The value given for $\langle 110\rangle$ in the (111) plane is taken from data at temperatures where the neck signal, which has a measured scattering rate nearly 20 times greater, has little effect. The point then meets the clean-signal requirement and its uncertainty is treated accordingly.

COMPARISON TO TFE AND RFSE

The comparison of the results obtained from this experiment to those from RFSE (Refs. 6 and 7) and TFE (Refs.

10 and 11) experiments is very interesting but presents some difficulties. The only other point determination of the electron-phonon scattering rate anisotropy in Ag is that reported in Ref. 10. Here the TFE signals were interpreted to give a measurement of $\gamma(\mathbf{k})$ [$\beta(\mathbf{k})$ in Ref. 10] at several points in the (100) zone. Each point of the TFE measurements actually represents an average over an angular range which we estimate to be on the order of $\pm 3°$. The TFE results were obtained from data taken at 45 GHz and should be directly comparable to ours obtained near 35 GHz. We have reproduced these points in Fig. 1 from the plot given in Ref. 10.

An inspection of the TFE and SLLR points in Fig. 1 shows that where they overlap near 5° and 10° in the (100) zone, they agree to well within experimental uncertainty. This supports our previous conclusion that the angular range of the effective strip around any extremal point is on the order of a few degrees. The point near 4.6° measured in TFE has an angular range of about ± 3. If the angular range corresponding to our 4.6° measurement were much larger than this, it would be an average over the large anisotropy near $\langle 100 \rangle$ and would give a smaller value than the TFE result. Considering the close correspondence between the two experimental results in the regions where they both apply, we feel that the TFE and SLLR measurements taken together provide a very clear point map of the anisotropy in $\gamma(\mathbf{k})$.

In comparing the SLLR and point TFE results to those obtained from inversion of orbit average measurements from TFE (Ref. 11) and two separate RFSE experiments,[6,7] several factors have to be considered: (a) The adequacy of the functional forms used in the inversion procedures. (b) The energy to which the electrons are excited by the experiment prior to their being scattered. (c) The extent to which the measurement technique samples the energy distribution of the electrons in the $\pm k_B T$ interval around the Fermi energy.

We will discuss each of these considerations in turn and point out some inconsistencies in arguments that have been made in previous comparisons.

(i) The TFE experiments can be analyzed in two ways. By taking the amplitude differences between successive TFE signal peaks, the point measurements given in Fig. 1 are obtained although the amplitude of an individual peak results from a much longer orbit average of the scattering frequency. In Ref. 11, Gasparov *et al.* have used these longer orbit averages as data in an inversion procedure to obtain an analytical expression for the anisotropy of $\gamma(\mathbf{k})$. The anisotropy obtained in this manner is also given in Fig. 1. Since the present SLLR results agree with the point TFE result while the orbit-average inversion falls below these values, we conclude simply that the number of terms used in this symmetrized Fourier expansion (5) is not sufficient to represent the magnitude of the anisotropy in $\gamma(\mathbf{k})$. While a small number of terms (five or seven) is perfectly adequate to represent the small variations from a constant encountered in Fermi radii ($\pm 10\%$), it is not sufficient for the order-of-magnitude variation in $\gamma(\mathbf{k})$.

(ii) The SLLR and the TFE measurements were made at microwave frequencies, with $\hbar\omega \simeq k_B T$, whereas the RFSE measurements are in the MHz range, where $\hbar\omega \ll k_B T$. The electrons contributing to conduction processes in a metal are distributed in energy over a range of $\sim 2k_B T$ around the Fermi energy and are expected to have a sharply-energy-dependent scattering rate[17] with the minimum scattering rate occurring at the Fermi energy E_F. Both of the microwave measurements accelerate electrons to energies above the equilibrium Fermi distribution at any temperature in the few Kelvin range. However, since electrons at any energy near the top of the equilibrium distribution can be raised into the excited state by this constant energy excitation, an energy distribution in the excited state resembling that of the equilibrium distribution, but centered around an average energy $E_{\text{av}} = E_F + \hbar\omega$ is expected. We assume that the energy averaged $\gamma(\mathbf{k})$ for this distribution is the same as that of the equilibrium distribution. The RFSE measurements, on the other hand, sample electrons within the equilibrium distribution and do not disturb it significantly. Thus, the SLLR and TFE results are expected to occur from a distribution of electron energies centered at a slightly different energy from the RFSE results but nevertheless having the same $\gamma(\mathbf{k})$.

(iii) The final question is to what extent the various experiments sample the thermal energy distribution of scattering rates. Since electrons at the center of the distribution are expected to have the longest times between scattering events (lowest γ), in both RFSE measurements attempts have been made to make measurements on only these electrons. The RFSE requires that an electron traverse the sample thickness at least once in order to contribute to the signal. By making the sample sufficiently thick, only electrons near E_F should contribute. Gasparov[6] made measurements on the thickest samples in which signals could be observed (~ 0.8 mm), while Johnson *et al.*[7] made thickness-dependent measurements and extrapolated the results to infinite thickness. The results of these two measurements are quite different with variations of 50% occurring for various orbits. Gasparov *et al.*[11] have argued that the extrapolation procedure is not valid and should lead to temperature-dependent linewidths. However, we have reexamined the data of Ref. 7 and find that all linewidths from the thinnest samples, where the largest temperature dependence would be anticipated, are the same to within experimental uncertainty at all temperatures. It may be that the thick samples used in Ref. 6 are not sufficiently thick to yield values of γ at E_F, but give values somewhere in between γ_{E_F} and the thermally averaged value. If this is correct, then for samples of this thickness departures from a T^3 behavior should be observed. Recent high-precision measurements of the RFSE amplitudes on samples even thicker than those used in Ref. 6 show this non-T^3 behavior.[18] Since the values given in Ref. 7 are from extrapolations to infinite thickness, they give γ_{E_F}.

In the SLLR a complete thermal average of the energy distribution being sampled is measured[19] since mean free paths in these experiments are always longer than a single skipping orbit. This is apparent in our experimental spectra since all but one of our measurements were made on (1-2) transitions and the (1-3) and (1-4) transitions were observable at all temperatures even though they have longer skipping orbit trajectories. On the other hand the

TFE again requires the electrons to traverse the sample thickness for a signal to occur. The measurements of Refs. 10 and 11 are stated to be in a limit of sample thickness such that again only the longest lived electrons contribute to the signal. As can be seen from Fig. 1, however, the results of the SLLR and point TFE measurements are the same. Thus it appears that even on moderately thick samples the TFE measures a completely thermally averaged scattering rate.

What is in question here is the definition of the thick-sample limit. The definition that has been used is that the sample thickness d should be greater than λ, where λ is the total mean free path of the electrons contributing to the signal. It appears instead that what is required to measure γ_{E_F} directly is that $d \gg \lambda$ and that this condition was not achieved with the apparatus of the sensitivity used in the TFE measurements, or in the RFSE measurements of Ref. 6.

For d less than the thick-sample limit, electrons with energies different from E_F contribute significantly to the signal, and thermal averaging effects are evident. The magnitude of the effect of thermal averaging on the measured values of $\gamma(\mathbf{k})$ depends on the degree to which d fails to meet the thick-sample criterion, $d \gg \lambda$, and on the details of the experiment. The RFSE and TFE are similar only in that electron trajectories on the same part of the FS contribute to the measured signal amplitude. In the RFSE the contribution of a particular electron to the signal depends on the number of half-orbits it completes, and this depends on the electron energy within the thermal distribution. An electron at E_F can have a mean free path more than twice that of one at the extremities of the distribution. Thus, the total contribution, including multiple passes, to the signal amplitude from an electron at a given energy depends on the electron lifetime at that energy. If d is such that electrons away from E_F contribute to the signal, the measured $\gamma(\mathbf{k})$ is a weighted average of the scattering rates of the contributing electrons. Thus, the mean free path for these experiments cannot be considered to be a simple mean, but rather it is a mean of the mean path at each energy.

In the TFE, however, conditions are quite different. The observed signals result from what are called type-II orbits in which electrons strike each surface of the metal at relatively large angles of incidence and are scattered diffusely. Electrons in these orbits are not expected to complete more than one transit of the sample regardless of their lifetime. The weighting of the thermally averaged scattering rate is different than in RFSE since all electrons whose lifetimes are such that they have a high probability of crossing the sample once make an essentially equal contribution to the signal amplitude. This difference may explain the variation in the scattering rates obtained in RFSE and TFE measurements on the same samples.

The Fermi surface of Ag is nearly spherical except for small regions near the necks. For a spherical FS the difference between the thermally averaged γ and γ_{E_F} should be a constant factor[17] of $\frac{7}{12}$. In Fig. 2 we give a point-by-point comparison of the SLLR and point TFE thermally averaged values of $\gamma(k)$ multiplied by $\frac{7}{12}$ to the values of $\gamma_{E_F}(k)$ obtained in Ref. 7 from an inversion of RFSE data extrapolated to $d=\infty$ orbit averages. As can be seen the agreement is reasonable at all points including the neck. As in the case of the TFE inversion the slightly lower ($\sim 10\%$) values from RFSE can be due to the small number of terms (4) used in this inversion. The RFSE values from Ref. 6 did not include orbits which extended into the neck region and so the inversion is not expected to be valid in this region. In the regions where it is valid the values of γ lie between the completely thermally averaged γ and γ_{E_F} at all points, indicating that these samples were not in the thick sample limit.

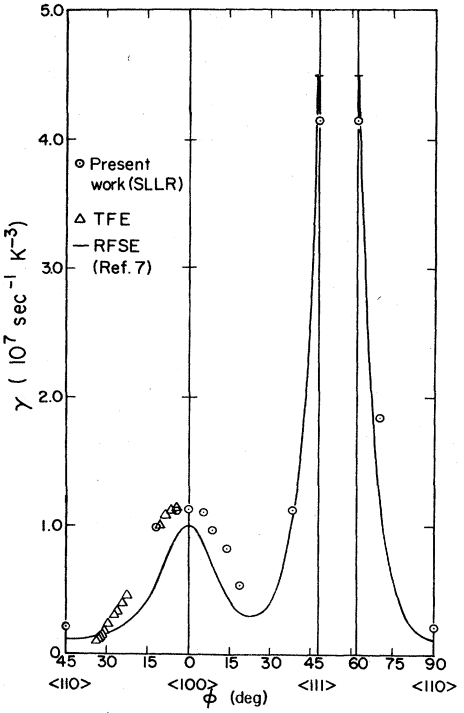

FIG. 2. Anisotropy of $\gamma(\mathbf{k})$ adjusted for the effects of thermal averaging. The solid line is the best four-term fit to RFSE data from Ref. 7. The SLLR and TFE points have been scaled by a factor of $\frac{7}{12}$.

SUMMARY

The results of the present experiment and previous experiments are as follows:

(1) The electron-phonon scattering rates in Ag are highly anisotropic and vary by a factor ~ 70 over the FS. This is shown in Fig. 1. Symmetrized Fourier expansion of orbit-averaged scattering rates using a small number of terms appear to be unable to reproduce the magnitude of this anisotropy.

(2) The results of different experimental techniques and conditions can be brought into agreement when the effects of thermal averaging over energy-dependent scattering

rates are properly taken into account.

(3) The difference between thermally averaged scattering rates and values at the Fermi energy on this nearly spherical FS is approximately $\frac{7}{12}$, as expected theoretically. This is shown in Fig. 2.

(4) Finally, the combination of the SLLR, TFE, and RFSE measurements provides an experimental determination of the electron-phonon scattering anisotropy in Ag in more detail than for any other metal.

ACKNOWLEDGMENT

This work was supported in part by the National Science Foundation under Grant No. DMR-82-06116.

[1]D. Nowak, Phys. Rev. B **6**, 3691 (1972).
[2]S. G. Das, Phys. Rev. B **7**, 2238 (1973).
[3]F. S. Khan, P. B. Allen, W. H. Butler, and F. J. Pinski, Phys. Rev. B **26**, 1538 (1982).
[4]V. F. Gantmakher and V. A. Gasparov, Zh. Eksp. Teor. Fiz. **64**, 1712 (1973) [Sov. Phys.—JETP **37**, 864 (1973)].
[5]P. B. Johnson and R. G. Goodrich, J. Phys. F **6**, L107 (1976).
[6]V. A. Gasparov, Zh. Eksp. Teor. Fiz. **68**, 2259 (1975) [Sov. Phys.—JETP **41**, 1129 (1976)].
[7]P. B. Johnson and R. G. Goodrich, Phys. Rev. B **14**, 3286 (1976).
[8]C. A. Steele and R. G. Goodrich, Phys. Rev. B **24**, 5576 (1981).
[9]R. E. Doezema and J. F. Koch, Phys. Rev. B **6**, 2071 (1972).
[10]V. A. Gasparov, J. Lebech, and K. Saermark, J. Low Temp. Phys. **41**, 257 (1980).
[11]V. A. Gasparov, J. Lebech, and K. Saermark, J. Low Temp. Phys. **50**, 379 (1983).
[12]J. W. Mitchell and R. G. Goodrich, preceding paper [Phys. Rev. B **32**, 4969 (1985)].
[13]R. E. Doezema and J. F. Koch, Phys. Kondens. Mater. **19**, 17 (1975).
[14]R. E. Prange, Phys. Rev. **187**, 804 (1969).
[15]T. W. Nee, J. F. Koch, and R. E. Prange, Phys. Rev. **174**, 758 (1968).
[16]J. F. Koch, Phys. Kondens, Mater. **9**, 146 (1969).
[17]D. K. Wagner and R. Bowers, Adv. Phys. **27**, 651 (1978).
[18]P. A. Probst, R. Stubi, R. Huguenin, and V. A. Gasparov, in *Proceedings of the 17th International Conference on Low Temperature Physics,* edited by U. Eckern, A. Schmid, W. Weber, and H. Wuhl (North-Holland, Amsterdam, 1984), Vol. II, p. 139.
[19]T. Wegehaupt and R. E. Doezema, Phys. Rev. B **18**, 742 (1978).